Violating The CHSH Inequality Using Entangled Photons

Author: Arjun Kudinoor
Partner: Aswath Suryanarayanan
Columbia University - PHYS 3081 Intermediate Physics Laboratory

(Dated: October 29, 2022)

The 2022 Nobel Prize in Physics was awarded to Aspect, Clauser, and Zeilinger for their "experiments with entangled photons, establishing the violation of Bell inequalities and pioneering quantum information science" [1]. In this paper, we describe our own experiment to violate the CHSH inequality - a type of Bell inequality - using entangled photons. We used the qutools quED Entanglement Demonstrator apparatus to generate entangled polarized photons using spontaneous parametric down-conversion. We measured photon polarization in rotated bases and calculated CHSH correlation values of $|S| = 2.123 \pm 0.030 > 2$ for entangled photons and $|S| < 2$ for non-entangled photons. We also generated non-classical correlation curves that describe polarization-measurement coincidences over a continuous range of polarizer angles for entangled and non-entangled photons. Our results demonstrate the nonlocality of entanglement and elucidate a better understanding of non-classical correlations of polarization measurements on photon pairs.

I. INTRODUCTION

In 1935, Einstein, Podalsky, and Rosen published a paper [2] that claimed that quantum mechanics' description of reality was incompatible with relativity. A key observation they made was that entanglement violated the principle of locality - that physical measurements depend on the vicinity around the object upon which a measurement is being made. Quantum entanglement did not obey this principle, and so there was a paradox (called the "EPR Paradox"). They hypothesized the existence of "hidden variables" to reconcile this paradox. Then, in 1964, John Bell published a paper [3] in response to EPR's hidden-variable theory. Bell's paper showed that the hidden variable description of entanglement was incorrect and that entanglement is inherently nonlocal. This was done by examining the correlation between measurements of entangled particles. A hidden variable theory would predict bounded correlations, yielding what is called a "Bell inequality". If correlations between measurements of entangled particles violated this inequality, then entanglement is a nonlocal phenomenon.

In our experiment, we demonstrate a violation of one type of Bell inequality - the CHSH inequality - using entangled photons. Polarization characterizes the 2-level quantum information of photons. Measuring the polarization of entangled photons in different bases allows us to calculate correlations between measurements. This allows us to test the CHSH inequality experimentally.

II. EXPERIMENTAL SETUP

A. The Apparatus

In this experiment, we used the qutools quED Entanglement Demonstrator [4] to demonstrate nonlocality of quantum entanglement using polarized photons. The quED Entanglement Demonstrator had two components: the laser source apparatus, and the polarizers and quCR unit. Within the laser source, as shown in Fig. 1, a laser diode pumped out ultraviolet photons that were linearly polarized in the vertical direction. The strongly divergent light from the laser diode is focused using a collimating aspheric lens and a negative spherical lens. After reflecting off of mirrors, the polarization of these photons is then adjusted with a half-wave plate. The half-wave plate alters the polarization of photons to yield equal amounts of horizontally and vertically polarized light. So, the state of a photon after encountering the half-wave plate may be written as

$$|\psi\rangle = \frac{1}{\sqrt{2}}(|V\rangle + |H\rangle) \tag{1}$$

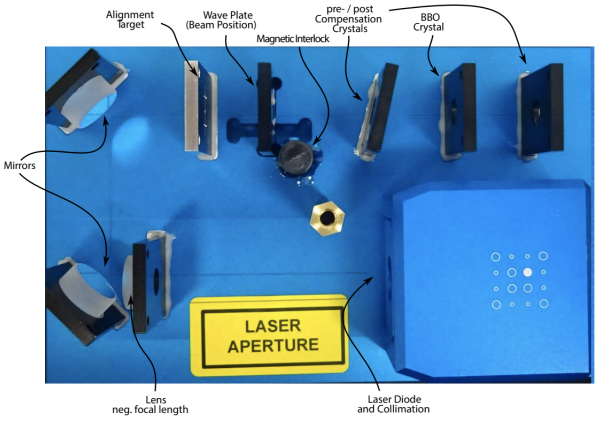

FIG. 1. qutools laser pump apparatus

The beam of photons then encounters a pre-compensation birefringent crystal, a nonlinear down-conversion crystal (BBO), and a post-compensation birefringent crystal. When the photons encounter the BBO

crystal, they undergo spontaneous parametric down-conversion (SPDC). In this process, horizontally polarized high-energy photons are split into two vertically polarized lower-energy photons, and vertically polarized high-energy photons are split into two horizontally polarized lower-energy photons.

$$|V\rangle \xrightarrow{\text{SPDC}} |H\rangle|H\rangle \tag{2}$$

$$|H\rangle \xrightarrow{\text{SPDC}} |V\rangle|V\rangle \tag{3}$$

Since equal parts of horizontally and vertically polarized light in Eq. 1 encounter the BBO crystal, the final state of photons post-SPDC is the entangled bell-state $|\Phi_+\rangle$.

$$|\psi\rangle \xrightarrow{\text{SPDC}} |\Phi_+\rangle = \frac{1}{\sqrt{2}}(|H\rangle|H\rangle + |V\rangle|V\rangle) \tag{4}$$

SPDC occurs with low probability - so most of the photons that exit the laser source apparatus are non-entangled high-energy photons. A long-pass filter is used to filter these high-energy photons out of subsequent sections of this experiment.

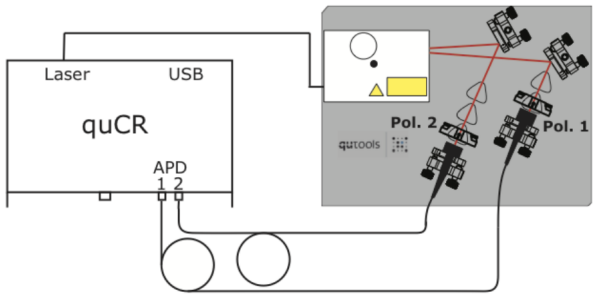

FIG. 2. Polarizers and quCR measurement apparatus

Once the entangled photons exit the laser source apparatus, they reflect off of two mirrors and encounter rotatable polarizers (as shown in Fig. 2). The polarization of each entangled photon is measured in a set of 16 rotated bases so that a correlation measure S (detailed below) between coincident photon measurements may be calculated by the quCR unit.

B. Theoretical Correlation Predictions

The two polarizers are rotated by angles of α and β. So, upon measurement, photons will occupy positive and negative polarization states in each basis: $|\pm_\alpha\rangle$ and $|\pm_\beta\rangle$, respectively. The probability of measuring two coincident photons in this basis is $P_{\pm\pm}(\alpha,\beta) = |\langle\pm_\alpha|\langle\pm_\beta|\psi\rangle|^2$. These probabilities are then used to calculate a measure of correlation

$$E(\alpha,\beta) = P_{++}(\alpha,\beta)+P_{--}(\alpha,\beta)-P_{+-}(\alpha,\beta)-P_{-+}(\alpha,\beta) \tag{5}$$

Theoretically, $E(\alpha,\beta) = cos(2(\alpha-\beta))$. The value of E in 4 sets of rotations $\alpha,\beta,\alpha',\beta'$ are measured to calculate a second measure of correlation

$$S = E(\alpha,\beta) - E(\alpha',\beta) + E(\alpha,\beta') + E(\alpha',\beta') \tag{6}$$

For a nonlocal theory of quantum mechanics - one with EPR's hidden variables -

$$\boxed{|S| \leq 2} \tag{7}$$

This is the CHSH inequality (one type of Bell's inequality). So, if $|S|$ is measured at values above 2, then the CHSH inequality is violated, and quantum entanglement is a nonlocal phenomenon. Theory predicts that for $(\beta-\alpha) = (\alpha'-\beta) = (\beta'-\alpha') = 22.5°$ and $(\beta'-\alpha) = 67.5°$, $|S|$ attains its maximum at

$$\boxed{|S|_{\max} = 2\sqrt{2} \geq 2} \tag{8}$$

So, theoretically, quantum entanglement is nonlocal. Our results below will demonstrate this experimentally.

III. RESULTS AND DISCUSSION

A. Discrete Correlations

We ran our experiment to measure correlations of entangled and non-entangled photons with varying lengths of integration time. Integration time corresponded to the periods of time over which photons could enter each polarizer - so, higher integration time yielded higher total photon counts for each measurement. Photons were entangled when the half-wave plate was inserted in the laser apparatus (in Fig. 1); the half-wave plate was removed to generate non-entangled photons.

Although the quCR unit calculated the correlation $|S|$ for us, I have included an explicit calculation of correlations E and errors dE for entangled photons with an integration time of 2000 ms in Table I.

For photon coincidence counts C, the correlation values E are given by

$$E(\alpha,\beta) = \frac{C(\alpha,\beta) - C(\alpha_\perp,\beta) - C(\alpha,\beta_\perp) + C(\alpha_\perp,\beta_\perp)}{C(\alpha,\beta) + C(\alpha_\perp,\beta) + C(\alpha,\beta_\perp) + C(\alpha_\perp,\beta_\perp)} \tag{9}$$

The errors dE in E were computed by gaussian error propagation

$$dE(\alpha,\beta) = 2\frac{(C(\alpha,\beta)+C(\alpha_\perp,\beta_\perp))(C(\alpha_\perp,\beta+C(\alpha,\beta_\perp))}{(C(\alpha,\beta)+C(\alpha_\perp,\beta_\perp)+C(\alpha_\perp,\beta)+C(\alpha,\beta_\perp)^2} \times \sqrt{\frac{1}{C(\alpha,\beta)+C(\alpha_\perp,\beta_\perp)} + \frac{1}{C(\alpha_\perp,\beta)+C(\alpha,\beta_\perp)}}$$

Then, the error in $|S|$ is

$$d|S| = \sqrt{\sum_{a=\alpha,\alpha';b=\beta,\beta'} (dE(a,b))^2} \tag{10}$$

Using Eq. 6 and 10, the data in Table I yielded

$$\boxed{|S| = 2.123 \pm 0.030} \tag{11}$$

We note that this is a value of $|S|$ above 2 with statistical significance. Thus, entanglement is nonlocal.

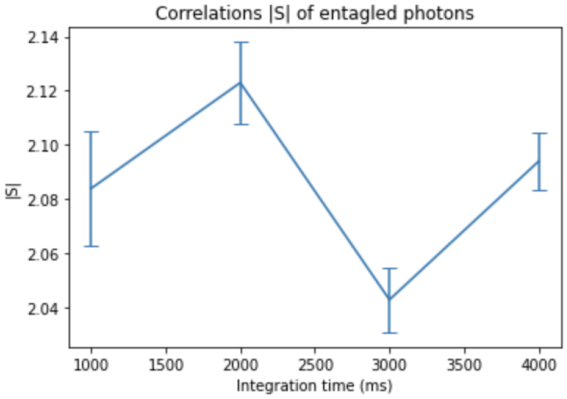

FIG. 3. Correlations $|S|$ of entangled photons vs. integration time with polarizer angles $\alpha, \alpha', \beta, \beta' = 0°, 45°, 22.5°, 67.5°$

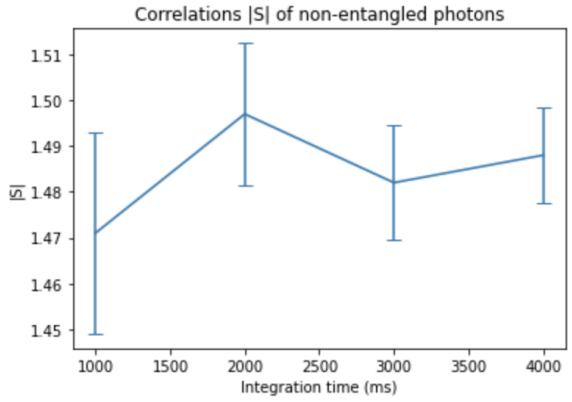

FIG. 4. Correlations $|S|$ of non-entangled photons vs. integration time with polarizer angles $\alpha, \alpha', \beta, \beta' = 0°, 45°, 22.5°, 67.5°$

We ran our experiment multiple times for different lengths of integration time with the same values of $\alpha, \alpha', \beta, \beta'$ as above. The results of these runs are depicted in Fig. 3 and 4. Although there was no statistical correlation between $|S|$ and integration time, the error $d|S|$ decreased as integration time increased. This was expected since higher integration times result in higher coincident photon counts and better statistics.

Values of S were consistently above 2 for entangled photons and below 2 for non-entangled photons, once again demonstrating the nonlocality of quantum entanglement. It is important to note that although the polarizer angles were chosen in such a way as to demonstrate maximum correlation $|S|_{\max} = 2\sqrt{2}$ (Eq. 8), our measurements did not attain this value. Misalignment and background noise from external light sources in the laboratory were major factors that caused of this discrepancy between prediction and measurement. These factors are discussed further in section IV.

B. Continuous Correlations

In addition to measuring coincidence counts, E, and $|S|$ for one set of specific angles $\alpha, \beta, \alpha', \beta'$, we also measured coincidence counts over a continuous range of angles. Keeping one polarizer (called the "static polarizer") at a fixed angle, we rotated the other polarizer (called the "dynamic polarizer") across a continuous angular range of $[0, 2\pi)$ while measuring and plotting the coincidence counts. After one full rotation, we rotated the static polarizer by 45° and repeated this process.

Fig. 5 and 6 show these (non-classical) coincidence correlation curves (simply, correlation curves) for entangled and non-entangled photons, respectively. The red curve was taken with the static polarizer set to horizontal, the blue one −45°, the yellow one vertical and the green one +45°.

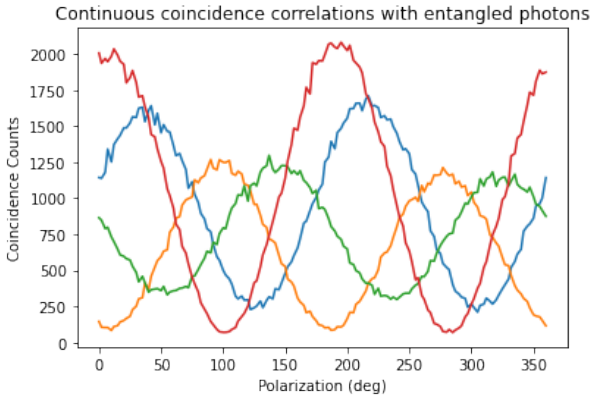

FIG. 5. Coincidence count vs. dynamic polarizer angle for entangled photons. The red curve was taken with the static polarizer set to horizontal, the blue one −45°, the yellow one vertical and the green one +45°.

We note that in the entangled case, photon pairs in the $|\Phi_+\rangle = \frac{1}{\sqrt{2}}(|H\rangle|H\rangle + |V\rangle|V\rangle)$ state enter the polarizers and should yield correlation curves of similar shape for each of the 4 static polarizer angles. The only difference between curves will be shifts by the corresponding rotations in the static polarizer. As described in [4], the

Pol. 1 (deg)	Pol. 2 (deg)	Coincidence Count (photons/second)	E	dE
0.0	22.5	1364	$E(\alpha,\beta) = 0.465$	0.016
0.0	112.5	324		
90.0	22.5	506		
90.0	112.5	911		
45.0	22.5	133	$E(\alpha',\beta) = -0.834$	0.010
45.0	112.5	1142		
135.0	22.5	1709		
135.0	112.5	125		
0.0	67.5	1185	$E(\alpha,\beta') = 0.434$	0.016
0.0	157.5	543		
90.0	67.5	368		
90.0	157.5	1122		
45.0	67.5	808	$E(\alpha',\beta') = 0.391$	0.017
45.0	157.5	336		
135.0	67.5	591		
135.0	157.5	1310		

TABLE I. Coincidence counts, calculated correlations E, and calculated errors dE for polarizer angles $\alpha, \beta, \alpha', \beta' = 0°, 22.5°, 45°, 67.5°$. Note that the coincidence counts in this table are the corrected coincidence counts calculated by the quCR unit after accounting for false coincidences.

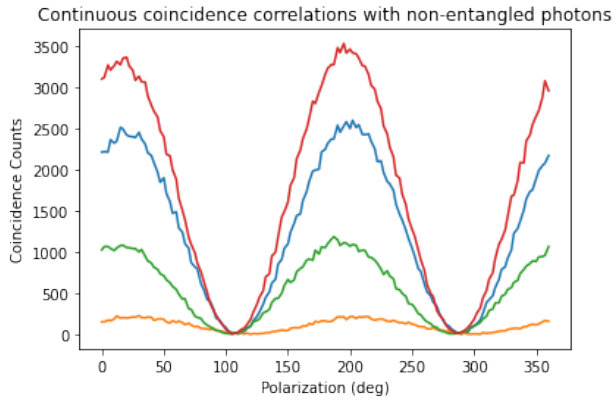

FIG. 6. Coincidence count vs. dynamic polarizer angle for non-entangled photons. The red curve was taken with the static polarizer set to horizontal, the blue one $-45°$, the yellow one vertical and the green one $+45°$.

coincidence probability (coincidence count divided by the total photon count) $P_a(b)$ for static polarizer angle a and dynamic polarizer angle b is

$$P_a(b) = \frac{1}{2} cos^2(a-b) \tag{12}$$

Although the correlation curves in Fig. 5 are cos^2-like, they have vastly different amplitudes. This is due to misalignments of the laser, mirrors, and polarizers in our experiment, as discussed in section IV.

In the non-entangled case, the half-wave plate is removed. So, a photon that is pumped out with vertical polarization $|V\rangle$ encounters the BBO crystals, splits into two photons via SPDC, and exists the laser apparatus with a state of $|H\rangle|H\rangle$. So, when measured by the polarizers, the amplitude of coincidence counts should be highest when both polarizers are horizontal, and lowest (almost 0) when both polarizers are vertical. In fact, if one of the polarizers is vertically oriented, then the coincidence count will be 0. This behavior is evident in Fig. 6, where the amplitude of the red curve (corresponding to a horizontal static polarizer) is largest, and the amplitude of the yellow curve (corresponding to a vertical static polarizer) is almost 0.

The 16 coincidence counts corresponding to the CHSH inequality are a subset of the points on the correlation curves. Table II details which curves correspond to each of the 16 angle pairs (a, b) where $a, b, \in \{\alpha, \beta, \alpha', \beta'\}$ involved in measuring the coincidence counts for calculating correlations $E(a, b)$ in Eq. 9. Since the calculation of correlations E depend upon the angles of the dynamic polarizer, so does the correlation measure $|S|$.

IV. CHALLENGES

During this experiment, we encountered multiple challenges. The most significant challenge was aligning the laser pump, mirrors, and polarizers accurately. In an ideal experiment the "singles" count rate of photons entering each polarizer would be 62,000 to 64,000 photons per second with coincidence counts of 5,000 photons per second [5]. Better alignment yielded higher singles count and coincidence count rates. However, there were 16 total degrees of freedom for us to manipulate during alignment. They consisted of 4 knobs on each of the two mirrors and the two polarizers. This made it incredibly tedious to align each of the elements in the qutools apparatus. However, after repeating the alignment procedure outlined in [4] multiple times, over a period of 3 weeks,

E	Pol. 1 (deg)	Pol. 2 (deg)	Correlation Curve
$E(\alpha, \beta)$	0.0	22.5	Red
	0.0	112.5	Red
	90.0	22.5	Yellow
	90.0	112.5	Yellow
$E(\alpha', \beta)$	45.0	22.5	Green
	45.0	112.5	Green
	135.0	22.5	Blue
	135.0	112.5	Blue
$E(\alpha, \beta')$	0.0	67.5	Red
	0.0	157.5	Red
	90.0	67.5	Yellow
	90.0	157.5	Yellow
$E(\alpha', \beta')$	45.0	67.5	Green
	45.0	157.5	Green
	135.0	67.5	Blue
	135.0	157.5	Blue

TABLE II. Correlation curves in Fig. 5 and 6 corresponding to angular pairs (a, b) where $a, b, \in \{\alpha, \beta, \alpha', \beta'\}$ involved in measuring the coincidence counts for calculating correlations $E(a, b)$. Here, Pol. 1 is the static polarizer, and Pol. 2 is the dynamic polarizer. The angle of Pol. 2 corresponds to the angle on the "Polarization (deg)" axis in Fig. 5 and 6

our best singles counts and coincidence counts were around 20,000 photons per second and 500 photons per second, respectively. Although this was much less than the ideal scenario, it was sufficient enough to yield correlation values of $|S|$ above 2 with statistical significance.

Another source of errors in our experiment was background noise from the environment. If light external to the laser pump entered the apparatus, it significantly increased the singles count and coincidence counts. Such external light sources included light inside the laboratory (ex: light fixtures in the room) and light from outside the laboratory (ex: sunlight). Increases in singles counts and coincidence counts from external light sources would yield inaccurate results. So, in all our trials of the experiment, we covered the entire apparatus in a black-box that shielded the apparatus from any external light.

V. CONCLUSION

In our experiment, we successfully violated the CHSH inequality Eq. 7 using entangled polarized photons and verified that non-entangled photons obey the CHSH inequality. We also generated correlation curves to measure coincidence counts of entangled and non-entangled photons. These curves agreed with theoretical predictions of coincidence probabilities for entangled and non-entangled photons. Finally, the coincidence counts corresponding to those involved in the CHSH inequality were identified as subsets of these correlation curves.

VI. FURTHER WORK

A natural next-step in this experiment is to improve the alignment of the laser, mirrors, and polarizer so that correlations closer to the maximum may be achieved. Another experiment is to measure $|S|$ over a continuous range of polarization angles, just as we measured coincidence counts and plotted correlation curves for a continuous range of polarization angles.

Experiments beyond this photon experiment to demonstrate violations of Bell inequalities would also be interesting. For example, one may violate Bell inequalities using techniques in quantum computing. In particular, one may encode a quantum algorithm to prepare entangled qubits (2-level quantum bits), measure their states in rotated bases using quantum gates, and calculate correlations $|S|$. I have implemented such an algorithm using the quantum computing platform Qiskit at [6]. The algorithm is tested on IBM's transmons-based `ibmq_quito` quantum computer. Just as this algorithm resulted in the development of other entanglement-based quantum algorithms, other experiments may reveal pathways for revolutionary applications of entanglement too.

VII. ACKNOWLEDGEMENTS

I would like to thank Professor Morgan May, Dacheng Xu, and all other TAs and mentors of this course for their guidance and support throughout this project.

[1] The Nobel Prize. Press release: The nobel prize in physics 2022. URL https://www.nobelprize.org/prizes/physics/2022/press-release/.

[2] A. Einstein, B. Podolsky, and N. Rosen. Can quantum-mechanical description of physical reality be considered complete? *Phys. Rev.*, 47:777–780, May 1935. doi: 10.1103/PhysRev.47.777. URL https://link.aps.org/doi/10.1103/PhysRev.47.777.

[3] J. S. Bell. On the einstein podolsky rosen paradox. *Physics Physique Fizika*, 1:195–200, Nov 1964. doi: 10.1103/PhysicsPhysiqueFizika.1.195. URL https://link.aps.org/doi/10.1103/PhysicsPhysiqueFizika.1.195.

[4] QuTools. qued: Entanglement demonstrator. URL https://www.qutools.com/files/quED/quED_manual.pdf.

[5] A. Lam, A. Holman, and W. Tom. Physun3081 spring 2021 intermediate laboratory work quantum entanglement and interference. URL http://www.columbia.edu/~mm21/exp_files/qentanglement_exp.pdf.

[6] A. Kudinoor. Quantum entanglement. URL https://www.arjunkudinoor.com/quantum/entanglement.